Carbohydrate Polymers 81 (2010) 790–798

Contents lists available at ScienceDirect

Carbohydrate Polymers

journal homepage: www.elsevier.com/locate/carbpol

Nano-in-micro alginate based hybrid particles

Abhijeet Joshi, R. Keerthiprasad, Rahul Dev Jayant, Rohit Srivastava*

Department of Biosciences and Bioengineering, IIT Bombay, AS Marg, Powai, Mumbai, Maharashtra 400 076, India

ARTICLE INFO

Article history:
Received 14 September 2009
Received in revised form 3 March 2010
Accepted 25 March 2010
Available online 3 April 2010

Keywords:
'Nano-in-micro'
Gelatin
$CaCO_3$
Alginate
Dexamethasone
LBL

ABSTRACT

Novel template containing 'Nanoparticles (gelatin and $CaCO_3$) embedded in Microspheres' ('Nano-in-micro') was developed using atomization. Dexamethasone loaded gelatin nanoparticles, fluorescein isothiocyanate–dextran (FITC–dex) loaded $CaCO_3$ nanoparticles and alginate based 'Nano-in-micro' system were prepared and characterized using optical microscopy, SEM, TEM, DLS, zeta potential, CLSM and FTIR. The results indicate that spherical, non-aggregating, 'nano-in-micro' particles (5–60 μm) can be prepared using atomization technique. Dexamethasone release from gelatin nanoparticles and 'nano-in-micro' systems indicated a decrease in burst release in the order: uncoated (24%) > coated (18%) > 'nano-in-micro' system (1:4 ratio) (17%). The sustained release decreased in order of 'nano-in-micro' (1:4 ratio) (14 days) > coated nanoparticles (9 days) > uncoated nanoparticles (4 days) for 95% drug release. FITC–dex loading and release from $CaCO_3$ nanoparticles were found to be molecular weight dependent. Thus, 'nano-in-micro' systems show possibility for use as drug release vehicles, biosensors and multifunctional systems.

1. Introduction

The development of hybrid nano/micro-particulate matrices has opened new avenues in basic, applied scientific research and industrial applications (Zheng & Gao, 2004). They are attractive for applications in pigment, paper, rubber, plastic industries and biomedical industry owing to their size, properties and capacity for spatial and temporal delivery of bioactives (Gorna & Hund, 2008; Volodkin & Petrov, 2004). Hybrid matrices often exhibit properties which are different from those of individual components enabling them to provide dual functionality. Several methods have been developed for the production of hybrid microspheres which include emulsion polymerization (Ma & Zhou, 2008), intercalative polymerization (Yang, Kong, Kan, & Sun, 1999), and hybrid latex polymerization (Tissot, Novat, Lefebvre, & Bourgeat-Lami, 2001). All these methods use surfactants and organic solvents, which are deterrent in toxicity.

Inorganic materials including silica, phosphates, carbonates of divalent and trivalent cations form the most common agents included in the preparation of hybrid matrices. Silica nanoparticles have been encapsulated in the interior spaces of PLGA and alginate/chitosan bio-polyelectrolyte microshells (Su, Tao, Xu, & Chen, 2007). Calcium phosphate–alginate composite microspheres have been used as enzyme delivery devices and as bone regeneration templates (Ribeiro, Barrias, & Barbosa, 2004). Incorporation of $CaCO_3$ in addition to improving the mechanical properties also provided an inert micro-environment for encapsulated biomolecules and drugs, making them useful for biosensor and drug delivery applications, respectively. It is also known to intensify the activities of enzymes in biosensors. $CaCO_3$/PMMA composites prepared by *in situ* emulsion polymerization have been previously described by Jian-ming, Yong-zhong, Zhi-ming, and Zhi-xue (2004). The abrasion resistant property of $CaCO_3$/poly(methyl methacrylate) (PMMA) nanocomposites was investigated by Avella, Errico, and Martuscelli (2001). Hollow chitosan–alginate coated carboxy methyl cellulose (CMC) doped $CaCO_3$ microspheres were loaded with doxorubicin for cancer therapy (Zhao et al., 2007). Similarly, polymeric nanoparticles of gelatin, alginate, polylactide-co-glycolic acid (PLGA), polylactic acid (PLA), and chitosan have also been used as a viable option for delivery of drugs (methotrexate (Casone, 2002), doxorubicin (Cameroni, 1999), cycloheximide (Saxena, 2005), paclitaxel (Lu, Yeh, Tsai, Au, & Wientjes, 2004), and chloroquine phosphate (Bajpai & Choubey, 2006)), genes (Zwiorek, 2004), proteins (Wona & Kim, 2008), antibodies and lymphocytes (Balthasar et al., 2005). Alginate has been widely used as a polysaccharide matrix for microsphere preparation. Being a well known biocompatible polymer, which ionically cross-links to form a gel in the presence of multivalent cations, it has certain advantages over other biocompatible matrices including slow and reproducible degradation rates, relatively inert aqueous environment within the matrix (Chavanpatil, Khdair, & Panyam, 2007; Rahman et al., 2006; Tonnesen & Karlsen, 2002), mild

* Corresponding author. Tel.: +91 22 25767746; fax: +91 22 25723480.
E-mail address: rsrivasta@iitb.ac.in (R. Srivastava).

0144-8617/$ – see front matter © 2010 Elsevier Ltd. All rights reserved.
doi:10.1016/j.carbpol.2010.03.050

room temperature gelation process and being free of organic solvents. The simplicity of process has led its widespread use in the incorporation of biomolecules without loss in biological activity.

Conventionally, alginate microspheres have been produced using external or internal gelation by dropping technique (Connick, 1983), emulsification (Lencki et al., 1989) and atomization methods (Stormo & Crawford, 1992; Sheu & Marshall, 1993). The atomization technique can be considered as most preferred technique owing to capability of forming small microsphere size, scale up and reduction in reagents required for the process (like surfactants and oils). Droplet generators have been used for producing polysaccharide microspheres which are either based on electrostatic field (Bugarski, Smith, Wu, & Goosen, 1993; Moghadam & Samimi, 2008) or air driven mechanism (De Vos, De Haan, & Van Schilfgaarde, 1997; Kwok, Groves, & Burgess, 1991). The process can be scaled up for industrial applications by developing air driven multi-needle droplet generators (De Vos et al., 1997). Their size can be modulated depending on the diameter of the jacket, the air flow rate, and the outer diameter of the nozzle, whereas the production rate depends upon the pressure on the alginate, and on the diameter and the length of the nozzle.

This research aims at developing a novel 'Nanoparticles embedded in Microspheres' (nano-in-micro) system comprising of nanoparticles embedded or entrapped in a polysaccharide based microspheres. The encapsulated nanoparticles can contain either a drug or macromolecules encapsulated/adsorbed/confined within them. This technique offers unique properties for implantable systems wherein the advantages of a nanoparticulate system including increased surface area is combined with that of microparticulate systems offering protection from reticulo-endothelial system and increased retention time, while on the other hand it offers the possibility of creating multifunctional systems containing components of different properties in different compartments. A novel method has been used for generating this nano-in-micro system in which a commercial air driven atomizing droplet generator was used. $CaCO_3$ nanoparticles and gelatin nanoparticles were part of the current study. While, $CaCO_3$ nanoparticles were loaded with a model macromolecule [fluorescein isothiocyanate–dextran (FITC–dex, 70 kDa)], the gelatin nanoparticles on the other hand, were loaded with an immunomodulating drug, dexamethasone. Layer-by-layer (LBL) assembly was used to control the release of entrapped materials from the systems. The drug release and macromolecular release from the nano-in-micro system was compared against uncoated and LBL coated nanoparticles.

2. Experimental

2.1. Materials

Gelatin [300 bloom (type A, from porcine skin) having mol. wt. of 87.5 kDa], alginate (low viscosity, 2%), sodium poly(styrene sulfonate) (PSS, 70 kDa), poly(allylamine hydrochloride) (PAH, 70 kDa), glutaraldehyde (25% solution), dexamethasone phosphate disodium salt (mol. wt. 392.5), sodium azide, phosphate buffer saline tablets, fluorescein isothiocyanate–dextran (FITC–dex) (70 kDa) were purchased from Sigma–Aldrich (India). Calcium chloride ($CaCl_2$) and sodium carbonate (Na_2CO_3) were purchased from Merck Ltd., Mumbai, India. Dialysis membrane (molecular cut-off 10–14 kDa) was purchased from Hi Media Laboratories, India. Analytical reagents like acetone, HCl, NaOH and NaCl were purchased from SD Fine Chemicals, India. MilliQ water having resistance less than 18 mΩ was used in all process of preparation and washing of particles. All chemicals were analytical reagent grade and were used as received.

2.2. Preparation of nanoparticles

Gelatin nanoparticles were prepared from a modified protocol of two-step desolvation method as developed by Azarmi (2006). Briefly, 25 ml of 5% gelatin solution was prepared at ambient temperature. Addition of equal volume of acetone to gelatin solution leads to the formation of desolvated gelatin which could be sedimented. The desolvated gelatin was redissolved in water and pH adjusted to 2.5. A second desolvation step was also carried out in order to prepare gelatin nanoparticles, process of which comprised of the addition of 75 ml acetone drop wise under constant stirring at 500 rpm. 250 μl of glutaraldehyde was added after 10 min to form cross-linked gelatin nanoparticles. Parameters like temperature, stirring speed, precipitation time and speed of acetone addition were optimized for the preparation of nanoparticles. Nanoparticle preparation employed the use of some optimized parameters including temperature (40 °C), stirring speed (500–700 rpm), precipitation time (90 s) and speed of acetone addition (3–5 ml/min). The formed nanoparticles were purified thrice by centrifugation (30,000 × *g* for 15 min) and re-suspension in acetone:water (70:30) mixture. The washed and purified nanoparticles were suspended in MilliQ water and stored at 4–8 °C.

$CaCO_3$ nanoparticles were prepared using precipitation from supersaturated solutions in the presence of PSS at ambient temperature as investigated by Joshi and Srivastava (2009). Briefly, 1 M Na_2CO_3 solution was rapidly poured into an equal volume of 1 M solution of $CaCl_2$ in the presence of 0.25% PSS in distilled water at room temperature with intense stirring and aged for 5 min. The particles so formed were thoroughly washed with de-ionized water and separated by centrifugation at 5200 × *g* for 10 min.

2.3. Preparation of nanoparticles loaded with actives

Dexamethasone sodium phosphate (0.2–0.5 mg/ml) was dissolved in water and mixed with desolvated gelatin polymer after first desolvation and precipitation. Second desolvation step was performed after drug loading as described in previous section. FITC–dex (70 kDa) (0.2 mg/ml) was mixed with preformed $CaCO_3$ nanoparticles and incubated for 10 min. The FITC–dex loaded $CaCO_3$ nanoparticles were purified by centrifugation at 5200 × *g* for 10 min and then washed to remove unloaded FITC–dex.

2.4. Preparation of nano-in-micro system

The nano-in-micro system was prepared using a commercial air driven droplet generator as shown in Fig. 1. The process involved mixing of nanoparticle suspension to a solution of 2% (w/v) sodium alginate. The nanoparticle–alginate suspension was then sprayed through an encapsulation unit or droplet generator (Nisco encapsulation unit Var J30, Zurich, Switzerland) optimizing several instrumental parameters (Nozzle diameter, flow rate, pressure, and distance of cross-linker solution from nozzle) and sample parameters (concentration of alginate, concentration of $CaCl_2$, ratio of nanoparticles, alginate, concentration of nanoparticles). The flow rate and pressure were monitored and fixed according to the in-built program of the syringe pump (Multi-Phaser™, model NE-1000, New Era Pump Systems, NY). Several optimization steps were carried out to fix the instrumental parameters like Nozzle diameter (0.35 mm) flow rate of solution/suspension (18–20 ml/h), pressure was maintained at (70–75 mbar) and distance of nozzle to cross-linking solution ($CaCl_2$) (10 cm). The fine spray of alginate solution/suspension was collected into 250 mM $CaCl_2$ solution for gelation under constant stirring (250 rpm) for 20 min. The loaded microspheres obtained were separated by centrifugation and washed using double distilled water.

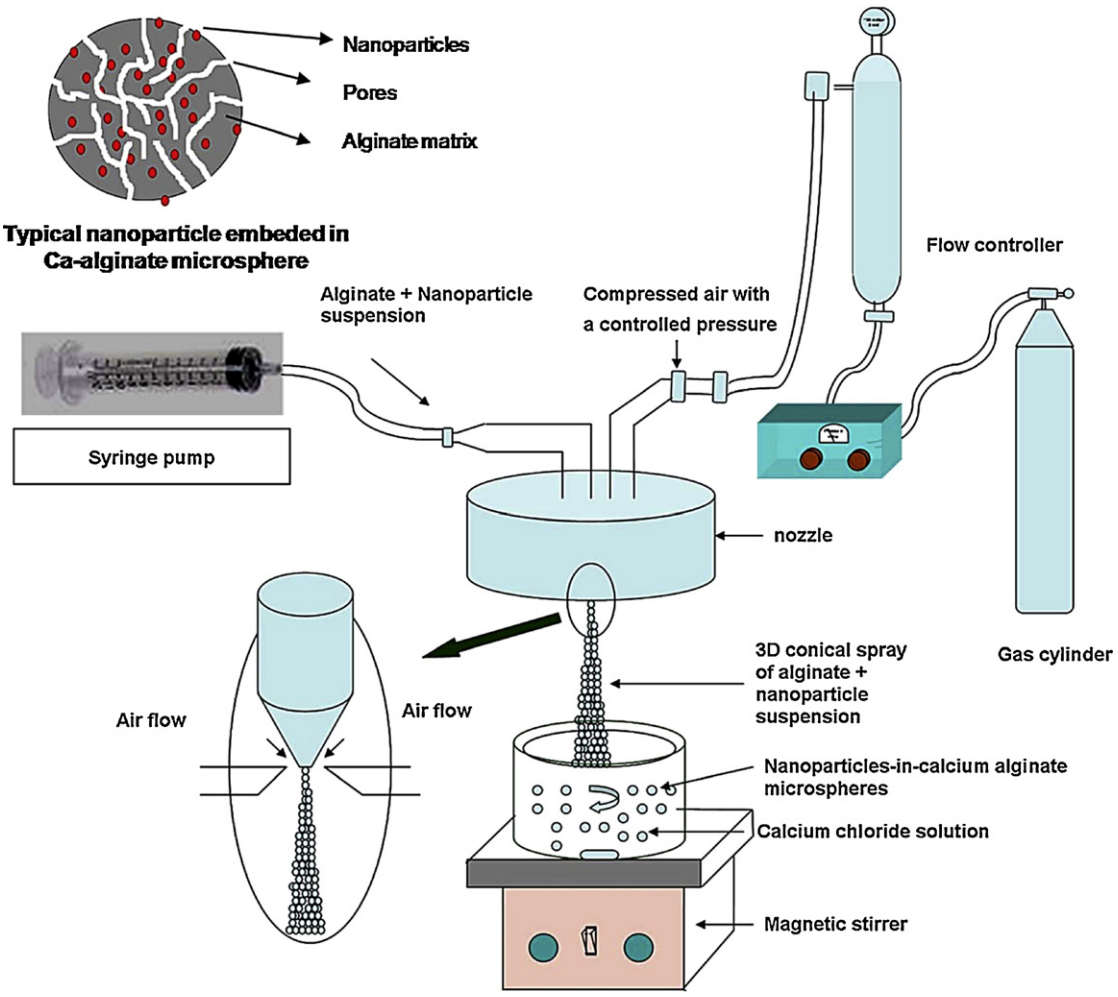

Fig. 1. Schematic diagram of instrument used for the preparation of nano-in micro particles using an air driven droplet generator.

2.5. Layer-by-layer (LBL) self-assembly on nanoparticles

Solutions of PAH (cationic), PEI (cationic) and PSS (anionic) were used for assembling $[PSS/PAH]_2$ and $[PSS/PEI]_2$ multilayers on $CaCO_3$ and gelatin nanoparticles, respectively. These polyelectrolytes were used at 2 mg/ml concentration prepared in 250 mM calcium chloride. Depending on the surface charge of the nanoparticles [i.e. PSS doped $CaCO_3$ (negative) and gelatin (positive)], they were first dispersed in oppositely charged polyelectrolyte in 2 ml of either PAH or PSS solution for 20 min, followed by two consecutive centrifugation and washing steps to remove excess polyelectrolyte. PSS–PAH coated $CaCO_3$ nanoparticles or PSS–coated gelatin nanoparticles were then suspended in PSS and PEI solutions, respectively. The reaction was allowed for 20 min prior to centrifugation and washing steps. The process was repeated to form $CaCO_3$ $[PSS–PAH]_2$ and gelatin $[PSS–PEI]_2$ assembly.

2.6. Particle size analysis

Samples including gelatin nanoparticles, PSS doped $CaCO_3$ nanoparticles, alginate microspheres and gelatin–alginate/$CaCO_3$–alginate (nano-in-micro system) microspheres system was examined at 10× using an optical microscope (Leica DMIL, USA) with a digital camera attachment. The particle size and morphology of the microsphere was studied using Leica image analysis software. SEM images of micro/nanoparticles were obtained by placing them on top of carbon tape, the samples were sputtered with gold using a gold sputter coater, and measurements were conducted at 150–3000× magnifications using accelerating voltage of 3 kV in a scanning electron microscope (Hitachi S-3400, Japan). TEM imaging of coated samples was carried out for morphological characterization. One-drop of freshly made coated micro/nanoparticles were added on carbon coated film copper grid. The samples were allowed to dry using an IR radiation drier for 1 h. The grids were then placed in the TEM (PHILIPS, CM200, USA) and viewed using an applied voltage of 200 kV. A small volume of nanoparticles was suspended in 1–2 ml of MilliQ water. Each sample measurement was reported as mean diameter analyzed in triplicate. Particle size distributions of nanoparticles were measured using DLS (Brookhaven Instruments, USA). The technique was based on the scattering of incident laser light due to the random Brownian motion of the nanoparticles which can be plotted as correlation function against time. The nanoparticles size distribution was calculated using mathematical contin algorithm depending on the environment of sampling and the temperature.

2.7. Zeta potential analysis

The electrophoretic mobility of the uncoated and LBL coated microspheres were measured using Zetaplus (Brookhaven Instruments, USA). The ζ-potential was calculated from the electrophoretic mobility (μ) using the Smoluchowski relation: $\zeta = \mu\eta/\varepsilon$ (where η and ε are the viscosity and permittivity of the solvent, respectively). For this experiment, 50 μl sample solution contain-

ing the microspheres was diluted in 2 ml of distilled water and used for analysis.

2.8. Confocal laser scanning microscopy (CLSM)

Fluorescent images of FITC–dex (70 kDa) loaded $CaCO_3$ nanoparticles were examined using confocal microscopy. Confocal micrographs of micro/nanoparticles were obtained with a flow view confocal laser scanning microscope (CLSM) equipped with a krypton–argon laser (Olympus FluoView™, Japan). An inverted microscope was also used which was equipped with an oil immersion objective lens (40×). The standard filter settings for fluorescence excitation (488 nm) and emission (520 nm) were used.

2.9. Fourier transform infra-red spectroscopy (FTIR)

Samples including gelatin nanoparticles, $CaCO_3$ nanoparticles, alginate microspheres, gelatin-in-alginate hybrid microspheres and $CaCO_3$-in-alginate hybrid microspheres were obtained in their dry form. Samples were thoroughly ground with dried KBr and discs were prepared by compression. FTIR analysis of the samples was performed using FTIR spectrometer (Nicolet Instruments Corporation, Magna 550, USA). Spectra were obtained on the spectrometer from 400 to 4000 cm^{-1}.

2.10. Encapsulation efficiency

The actual drug loading or encapsulation efficiency (% EE) (in percentage) in the gelatin nanoparticles was determined by calculating the difference between the total (W_{total}) and the free drug (W_{free}) concentrations in the nanoparticle suspension and the supernatant per mg of gelatin nanoparticle (M).

$$\%\,\text{drug loading} = \frac{W_{total} - W_{free}}{M} \times 100$$

2.11. Drug release studies

In vitro drug release studies were performed on uncoated nanoparticles, polyelectrolyte coated nanoparticles cross-linked and nanoparticle-in-alginate microspheres using a dialysis membrane with molecular weight cut-off of 10–14 kDa. Drug loaded uncoated, coated and microspheres were transferred to a beaker containing 200 ml of 0.01 M phosphate buffered saline (PBS, pH 7.4) and 0.01% (w/v) sodium azide. The samples (in duplicate) were incubated in a 37 °C incubator under sink condition for the release studies. At preset time intervals, the release medium was collected and replaced with a fresh buffer solution. The % cumulative release profiles were obtained by taking the ratio of the amount of drug released to the total drug content and were determined spectrophotometrically at λ_{max} of 242 nm. All measurements were performed for $n = 3$ samples.

3. Results and discussion

3.1. Preparation of nanoparticles

Desolvation process for preparing gelatin nanoparticles is a self-charge neutralization process where the positively charged segments in the chain overlap with the negatively charged segment of the same chain due to coulombic interactions causing charge neutralization. Acetone or ethanol is the commonly used desolvating agents. Two-step desolvation process was selected because since unlike other proteins like albumin, gelatin is a mixture of protein fractions of different molecular weights and different fractions precipitate at different degrees of desolvation. The first desolvation step involves the elimination of low molecular weight fractions and the second step is involves the actual formation of nanoparticles. The gelatin nanoparticles were formed largely through both inter- and intra-molecular electrostatic interactions. In the initial stages of nanoparticle formation occurs due the competition between intra-molecular folding and intermolecular aggregate formation. $CaCO_3$ nanoparticles on the other hand were prepared using precipitation by reaction of counter-ions showed aggregation phenomena to a size of 5–7 μm. The mechanism involved the formation of amorphous precipitate which transforms into microcrystal of different morphologies and sizes. However when PSS was added in the reaction mixture, small spherical particles with uniform size were formed having size 500 nm to 2 μm. The mechanism of reduction of size and formation of spherical nanoparticles can be explained on the basis of micellization effect of PSS. The nanoparticles were selected due to their suitability of encapsulation for macromolecules due to their mesoporous structure (Joshi & Srivastava, 2009; Kawaguchi et al., 1992).

3.2. Loading of actives and encapsulation efficiency

Drug loading of nanoparticles is defined as the amount of drug per mass of polymer whereas (mg of drugs per mg of polymer) encapsulation efficiency refers to ratio of amount of drug encapsulated to the theoretical loading amount used. Drug loading was determined indirectly by determining the concentration of dexamethasone which is free in the supernatant. The drug present in supernatant was determined using a standard curve prepared by UV spectroscopy at 242 nm. The regression equation $y = 4.698x - 0.047$ was plotted in range 0.02–0.5 mg/ml. Drug loading in gelatin nanoparticles was found to be 1.38, 1.26, 1.22, and 0.85% at 0.5, 0.4, 0.3 and 0.2 mg/ml concentrations, respectively. At 0.2 mg/ml the encapsulation efficiency was found to be very high (89.6%) while at 0.5 mg/ml efficiency decreased to about 58.6%. When the drug concentration increased from 0.2 to 0.3 mg/ml the efficacy decreased. Drug loading was found to be nearly constant till 0.3 mg/ml, however the efficiency is found to decrease drastically with further increase in concentration because of saturation. Similarly FITC–dex encapsulation in $CaCO_3$ indicated a high loading (64%) as shown by Joshi and Srivastava. The entrapment/encapsulation was found to be molecular weight dependent and increase in molecular weight reduced the entrapment efficiency. Further, use of LBL coatings has shown to reduce the leaching of FITC–dex to an extent of 51% after two bilayer coatings (Joshi & Srivastava, 2009).

3.3. Preparation of nano-in-micro particles

The droplet generator works on the principle of aerodynamic force where the sodium alginate solution while passing through the nozzle (diameter = 0.35 mm) breaks up into micron size particles as shown in Fig. 1. The optimization process as developed by Jayant and Srivastava (2007) was performed to obtain uniform sized alginate microspheres. Several instrumental parameters like nozzle size (0.35 mm), pressure (70–75 mbar), flow rate (10–18 ml/h), distance from nozzle to cross-linking solution ($CaCl_2$) (5–10 cm) were fixed after optimization using alginate solution (2%, w/v) sprayed in $CaCl_2$ (250 mM). The optimization study was performed according to a modified method acquired from Jayant and Srivastava. The average size of alginate microspheres using these optimized parameters was 60 ± 5 μm as demonstrated in Fig. 2(I) and (II) for the various conditions.

For nano-in-micro system, nanoparticles were mixed with alginate in two ratios (1:4 and 3:4 for gelatin nanoparticles and 1:4 and 3:4 for $CaCO_3$ nanoparticles) and used for microsphere preparation. Alternatively, changes in particle size were determined by changing few instrumental parameters. Detailed parameters which

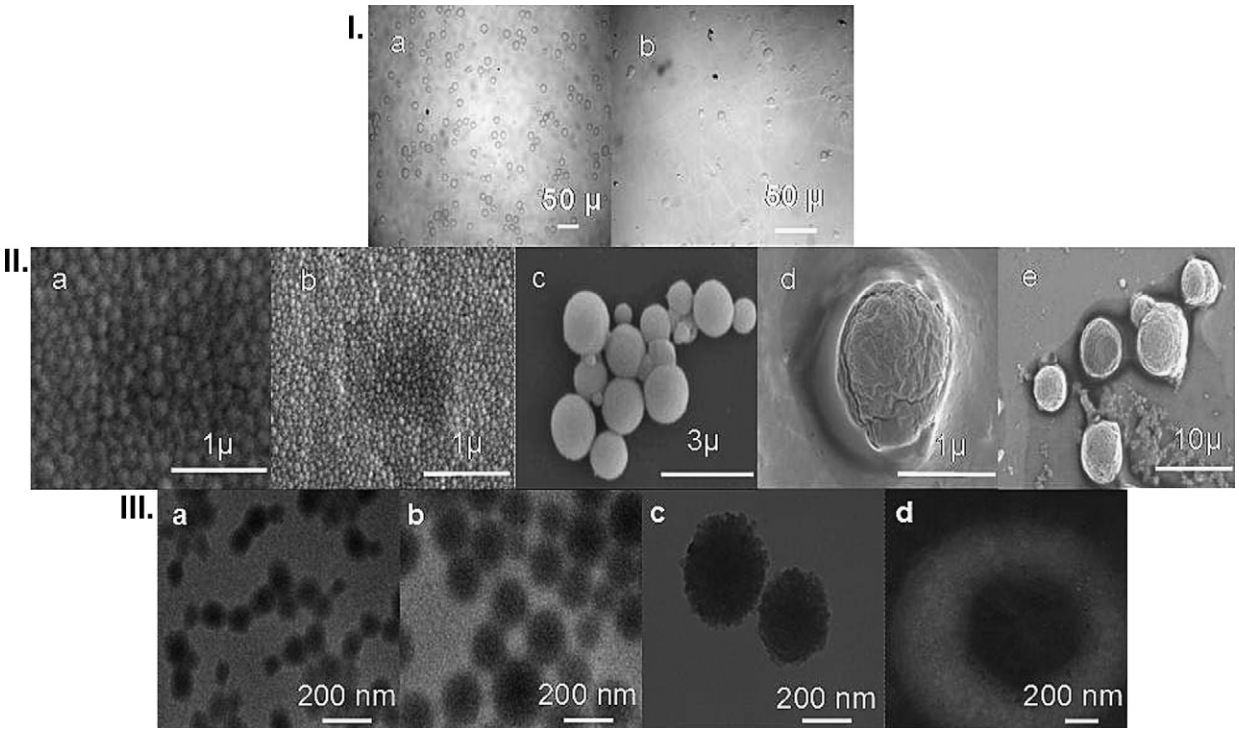

Fig. 2. (I) Optical images of (a) alginate microspheres and (b) 'nano-in-micro' system; (II) SEM images of uncoated gelatin nanoparticles (a), coated gelatin nanoparticles (b), uncoated $CaCO_3$ nanoparticles (c), coated $CaCO_3$ nanoparticles (d) and typical nanoparticles-in-alginate microspheres (e); and (III) TEM images of uncoated (a and c) and coated (b and d) nanoparticles of gelatin (a and b) and $CaCO_3$ (c and d).

were used and optimized have been listed in Table 1. During optimization the results as obtained by Jayant and Srivastava were validated for the preparation of alginate microspheres and these were used for the preparation of nano-in-micro particles. In general during optimization it was observed that increase in pressure lead to decrease in size, however sphericity was lost to some extent which could be counter-balanced by increase in flow rate. In addition to this when nanoparticles were mixed in alginate solution, smaller particle sizes could be formed, which are mainly due to the production of shear during atomization. Further, they also served to provide nuclei for the formation of droplets which in turn lead to the formation of smaller particles.

3.4. Particle size analysis

Microscopic images of alginate microspheres were found to be in the size range of 30–130 μm (Table 1) while nano-in-micro alginate microspheres were found to be spherical with size ranging from 5 to 60 μm depending upon the parameters optimized for spraying the suspension through an apparatus described in Fig. 1.

The SEM images of uncoated, coated and nano-in-micro particles of gelatin indicate that the particles formed are spherical in nature having diameter of 200 nm, 500 nm and 5–60 μm, respectively. On the other hand uncoated, coated and 'nano-in-micro' particles of $CaCO_3$ indicate that the size of particles ranged from 700 nm, 1, 2 and 5–60, respectively. The SEM results indicate a lower particle size than DLS due to drying effects during sample preparation (Fig. 2(II)). TEM images reveal perfectly spherical dispersed particles. The sizes as determined from TEM images suggest the particles to be between 180 and 220 nm for plain gelatin nanoparticles while PSS/PEI coated particles are around 500 nm. $CaCO_3$ nanoparticles were visible as dark, solid, mesoporous with channels and pores in the structure. LBL coating was not clearly visible in case of gelatin nanoparticles, because of their small size, but in case of $CaCO_3$, LBL coating (2 BL) can be seen around the $CaCO_3$ nanoparticles (Fig. 2(III)).

Particle size and size distribution of nanoparticles and LBL coated nanoparticles were determined by dynamic light scattering using Brookhaven's instruments for gelatin nanoparticles and Nicomp® particle sizing systems for $CaCO_3$ nanoparticles. Both the techniques are based on a deconvolution (contin) algorithm

Table 1
Optimization of parameters for the preparation of plain alginate microspheres and nano-in-micro particles. Values in parenthesis represent the standard deviation for triplicate measurements.

$C_{alginate}$ (%, w/v)	C_{CaCl_2} (%, w/v)	Nozzle size (μm)	Pressure (mbar)	Flow rate (ml/h)	Distance (cm)	Concentration nanoparticles: alginate	Size of nano-in-micro particles (μm)
1.5	200	0.35	150 (5)	130 (2)	5	–	130 (±10 μm)
1.5	200	0.35	130 (5)	110 (2)	5	–	120 (±10 μm)
1.5	200	0.35	110 (5)	90 (2)	5	–	100 (±10 μm)
2.0	250	0.35	90 (5)	70 (2)	5	–	80 (±10 μm)
2.0	250	0.35	55 (5)	30 (2)	5	–	60 (±10 μm)
2.0	250	0.35	70 (5)	20 (2)	10	–	60 (±10 μm)
2.0	250	0.35	60 (5)	10 (2)	10	1:4	60 (±10 μm)
2.0	250	0.35	120 (5)	10 (2)	10	1:4	25 (±5 μm)
2.0	250	0.35	300 (5)	15 (2)	10	3:4	15 (±5 μm)
2.0	250	0.35	500 (5)	15 (2)	10	3:4	8 (±5 μm)

Table 2
Particle size distribution analysis of uncoated, coated nanoparticles and nano-in-micro particles.

Sample	Size	Sample	Size
Gelatin nanoparticles (uncoated)	175 nm (0.07)	$CaCO_3$ nanoparticles (uncoated)	816 nm (0.49)
Dexamethasone loaded gelatin nanoparticles	201 nm (0.09)	–	–
$[PSS/PEI]_2$ coated gelatin nanoparticles	581 nm (0.12)	$[PSS/PAH]_2$ coated $CaCO_3$ nanoparticles	2 μm (±1 μm)[a]
Gelatin nanoparticles in alginate microspheres	5–60 μm (±10 μm)[a]	$CaCO_3$ nanoparticles in alginate microspheres	5–60 μm (±10 μm)[a]

Values in parenthesis represent the polydispersity index.
[a] Values in parenthesis represent the standard deviation.

for dynamic light scattering. Several distribution analysis methods such as intensity weighted, volume weighted and multimodal distribution analysis were applied. The results have been summarized in Table 2. A slight increase of ~25 nm in the mean diameter of gelatin nanoparticles was observed in comparison to uncoated unloaded gelatin nanoparticles. Further, on the addition of coating of $[PSS/PEI]_2$ the mean diameter increased to ~580 nm using similar parameters. $CaCO_3$ nanoparticles showed a mean diameter as determined by intensity distribution of particles was found to be 816 nm (0.49). A higher value of polydispersity indicates the aggregation of $CaCO_3$ nanoparticles due to a lower value of zeta potential (−7 mV).

3.5. Zeta potential measurement

Surface charge or zeta potential in case gelatin nanoparticles was largely dependent on the pH of the suspension. A study employing different pH ranges for the preparation of nanoparticles suggested that at extremes of pH gelatin nanoparticles showed finite values (negative and positive) for zeta potential, however when isoelectric point was approached the zeta potential values were reduced as shown in Fig. 3.

The effect of pH on the zeta potential of cross-linked gelatin nanoparticles was studied which suggested that as the pH increased the zeta potential values decreased approaching zero till the isoelectric potential. Zeta potential was found to be between +33 and −36 mV when pH was changed from 2.2 to 8.5. This can be explained by the fact that presence of ionisable amine groups NH_4^+ and carboxyl groups COO^-. At lower pH the amine groups are protonated which gives rise to a positive charge and at higher pH the carboxyl groups are deprotonated giving a negative charge to the particles. The isoelectric point is observed to be around pH 5.5 and the particle shows high surface potential around physiological pH making it a suitable matrix for drug administration. The surface charge of gelatin nanoparticles was found to decrease with dexamethasone loading to ~25 mV. This is evident because of the fact that phosphate salt of dexamethasone has been used which electrostatically neutralizes the positive charged amine groups. During the LBL assembly the zeta potential shifted from negative to positive on the addition of PEI and vice versa on addition the of PSS (Fig. 3). In case of $CaCO_3$ nanoparticles, preparation was performed in neutral pH conditions, $CaCO_3$ showed a slight negative charge leading to aggregation effects. In order to reduce these effects PSS was used so that the zeta potential could be increased on negative side. This formed the basis of build of subsequent nanofilms. Alternating negative and positive zeta potentials in gelatin and $CaCO_3$ nanoparticles confirmed the LBL assembly over nanoparticles.

3.6. CLSM

The fluorescent images of nano-in-micro system shown in Fig. 4 indicate FITC–dex loaded nanoparticles (appearing green in picture). (For interpretation of the references to color in text, the reader is referred to the web version of the article.) The punctuate marks of fluorescence indicate non-aggregated nanoparticles encapsulated in microspheres when compared against the DIC image. The fluorescent images and their corresponding DIC images show that the nanoparticles lie within the matrix. The sizes of the microspheres are more or less consistent regardless of the nanoparticles encapsulated within them. The particles appear spherical and well defined. The presence of the nanoparticles has not proved to be abrasive or structurally deforming. Fig. 4 depicts microparticle with loading of nanoparticles to see if any structural abnormality arises due to the encapsulation of increasing amounts of nanoparti-

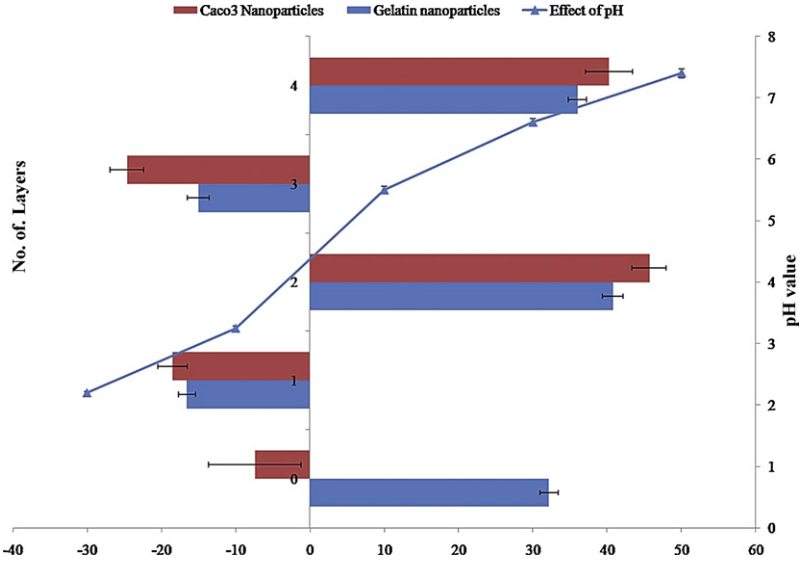

Fig. 3. Zeta potential measurement of gelatin (■) and $CaCO_3$ nanoparticles (■) during LBL assembly (represented by horizontal bars) and variation of zeta potential of gelatin nanoparticles due to changes in pH (-- ▲ --) (represented as line graph); *X* and *Y* error bars represent the standard error of mean values.

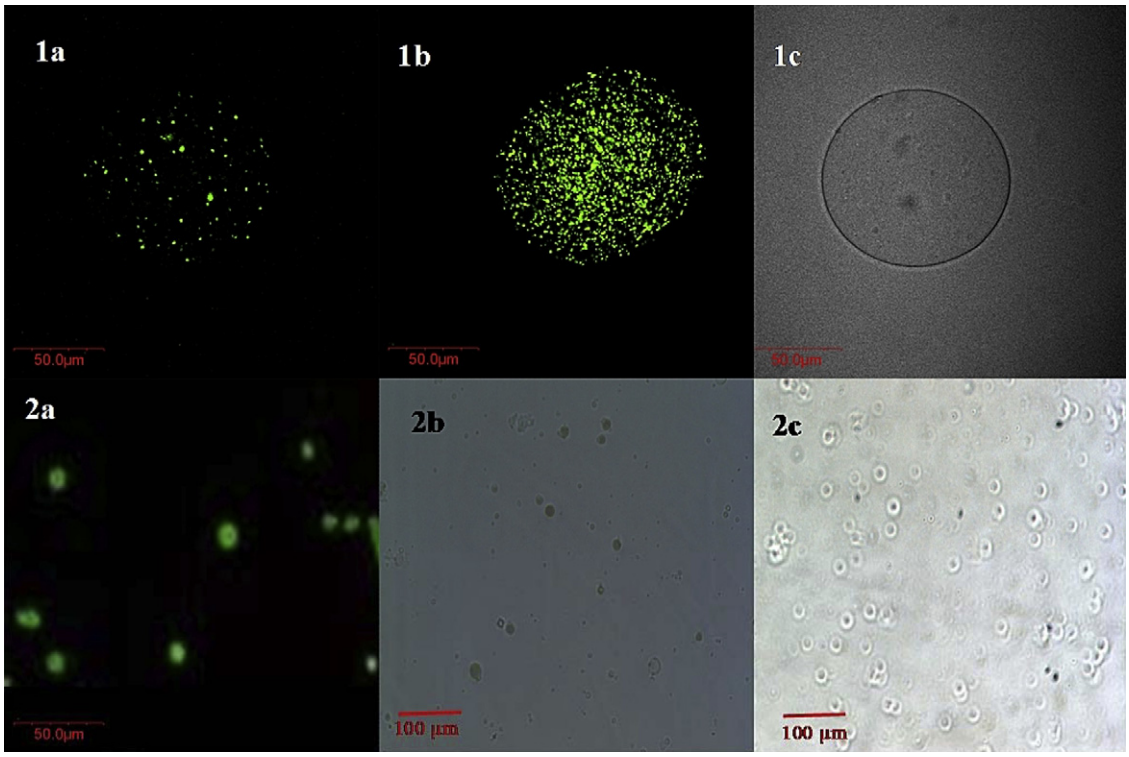

Fig. 4. CLSM images of FITC–dex loaded gelatin nanoparticles (1a), gelatin-in-alginate microspheres (1b) and $CaCO_3$ nanoparticles (2a), and $CaCO_3$-in-alginate microspheres (2b). Differential interference contrast images of gelatin-in-alginate microspheres (1c) and $CaCO_3$-in-alginate microspheres (2c).

cles. In case of $CaCO_3$ loaded with FITC dye, it was found that it was not retained in $CaCO_3$ nanoparticles due to mesoporous nature of $CaCO_3$. However when $CaCO_3$ was loaded with FITC–dex (70 kDa) it was found to be retained to a greater extent due to its high molecular weight and the adsorption of the macromolecule on the $CaCO_3$ nanoparticles.

3.7. FTIR

Gelatin being a proteinaceous molecule C=O and NH bond stretching vibrations act as an index of its presence. The peak at 3450 cm^{-1} which is indicative of N–H bonds present in gelatin was observed in both gelatin and gelatin-in-alginate hybrid microspheres. The peaks at 1400 cm^{-1} indicate CO bond stretching and as both gelatin and alginate contains these groups similar peaks are observed in the two graphs (Fig. 5). The major characteristic peak of CO stretching at 1400 cm^{-1} is due to the concentration of CO bond both in gelatin and in alginate leading to a sharp, high intensity peak. The characteristic peaks of gelatin and alginate also correspond to the research carried out by Bajpai and Choubey (2006) and Wang, Chen, Ye, and Hu (2008).

On the other hand, $CaCO_3$ nanoparticles show peaks at 3442, 2925, 1490, 1437, 877 cm^{-1} (Gorna & Hund, 2008; Ma & Zhou, 2008). In case of $CaCO_3$-in-alginate hybrid microspheres, two peaks (1437 and 877 cm^{-1}) characteristic of $CaCO_3$ nanoparticles were observed indicating the presence of $CaCO_3$ in the hybrid microspheres (Fig. 5) The peak at 1437 cm^{-1} becomes more prominent and sharp due to the synergistic effect of C=O of $CaCO_3$ and alginate. Due to a higher concentration of alginate in $CaCO_3$-in-alginate particles the OH stretching peak at 3400 cm^{-1} appears broadened. FTIR studies indicate that in both systems containing gelatin-in-alginate and $CaCO_3$-in-alginate no new peaks corresponding to any chemical bonding arise but the presence of characteristic peaks of components shows that both the components are physically present in the matrix. The reduced intensities of peaks corresponding to $CaCO_3$ and gelatin in hybrid nano-in-micro system are due to lower concentration ratios in the microspheres.

3.8. Drug release studies

In release studies, release profiles of uncoated nanoparticles, LBL coated nanoparticles (1 bilayer (1 BL) and 2 bilayer (2 BL)), nano-in-micro hybrid particles containing (1:4 and 3:4 loading of nanaoparticles:alginate) were compared as shown in Fig. 6. Gelatin nanoparticles showed zero order release behaviour for dexamethasone after an initial burst release period which lasted for 3 h. During the burst release period up to 25% of the drug was released.

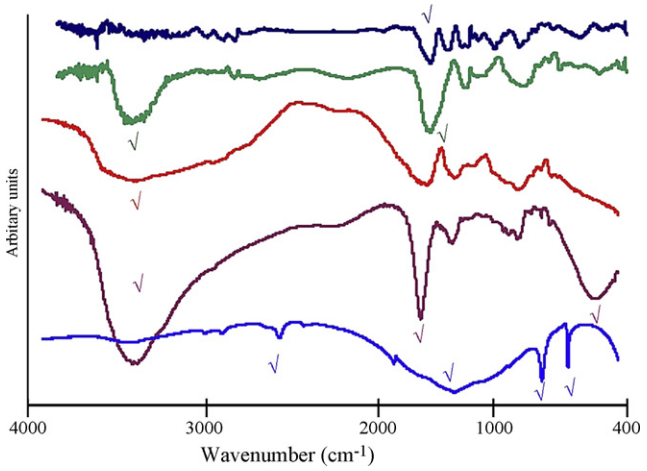

Fig. 5. FTIR spectra of $CaCO_3$ nanoparticles ( ), gelatin nanoparticles ( ), alginate microspheres ( ), gelatin-in-alginate hybrid microspheres ( ) and $CaCO_3$-in-alginate hybrid microspheres ( ).

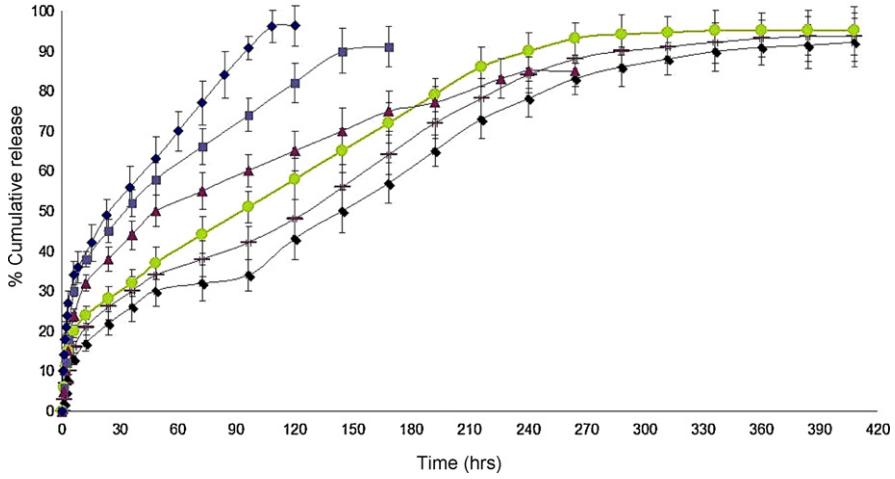

Fig. 6. Drug release studies for uncoated nanoparticles (-◆-), coated nanoparticles [1 BL (-■-), 2 BL (-▲-)], alginate microspheres (-●-), nano-in-micro [1:4 (-◆-), 3:4 (-||-)]. *Y* error bar represents the standard deviation for triplicate measurement.

Following the burst release a steady zero order release kinetics up to 4 days was observed with a correlation coefficient of 0.994. The biphasic pattern of drug release is characteristic of matrix diffusion kinetics, as is expected in a nanoparticles based drug delivery system. 97% of the initial drug loading was found to be released in the duration of 96 h. LBL coated (2 BL) nanoparticles showed reduced burst release from the nanoparticles. This could be attributed to a decrease in surface associated drug in LBL coated particles. 2 BL coated particles released only 15% of the drug in contrast to 18% of the 1 BL coated particles in first 3 h. The sustained release of drug after the burst release lasted for 6 days in the 1 BL coated particles, releasing 90% of the initially loaded drug. However in the case of 2 BL coated particles the release was could be sustained up to 9 days showing 85% of initial loading. The release of dexamethasone could be prolonged to an extent of 50 and 100% in 1 BL and 2 BL coated nanoparticles, respectively. This increase in the release period is due to the presence of an additional diffusion layer which acts as a barrier.

The comparison of release profiles of nano-in-micro systems (1:4 and 3:4 ratios) against plain alginate microspheres shows that initial burst release was 21 and 17% in the case of 1:4 and 3:4 configurations, respectively. The initial burst release was clearly reduced when compared against plain alginate microsphere wherein 24% of dexamethasone was released during burst release period. This is attributed to the lack of surface adhered drug alginate microspheres containing nanoparticles. The immediate reservoir of drug is in the open pores of the alginate matrix which can be diffuse out instantaneously. Lower percentage of burst release is indicated due to this phenomenon in both the nano-in-micro configurations. The sustained release phase of the three configurations (plain alginate microspheres, 1:4 and 3:4 nano-in-micro systems) showed significant differences in the release pattern. The plain drug loaded alginate particles show a normal zero order release profile, as expected; the nano-in-micro systems showed a varied release profile. Both the nano-in-micro system showed a decrease in % cumulative release during 96–100 h, after which it follows a regular zero order kinetics. This variation from the normal zero order profile can be explained by the presence of two different matrices in a single system which individually exhibit different release profiles. In both the nano-in-micro configurations, the drug released from nanoparticles is not held by the alginate matrix, but instead the drug only diffused through the pores of the alginate matrix. As it was observed that gelatin nanoparticles released its contents in a 4 days period, after 4 days, the alginate pores in the matrix holds the drug in the form of a reservoir after gelatin is degraded. The nano-in-micro system prolonged the release up to 14 and 16 days in case of 1:4 and 3:4 systems, respectively when compared against drug loaded alginate microspheres which maintained release for 11 days. This showed superiority of the nano-in-micro system over other nanoparticle and microparticle matrix based drug delivery systems in terms of reduced burst release and prolonged release.

4. Conclusions

Novel nanoparticles embedded in microspheres (nano-in-micro) have been prepared and optimized. The method based on the air driven atomization can be used as a platform technology for the encapsulation of nanoparticles in alginate based microspheres. Microsphere production was achieved by cross-linking of atomized droplets of alginate containing nanoparticles. Various sizes ranging from 5 to 60 μm can be achieved by the alteration of instrumental and sample parameters. Encapsulation of drug loaded nanoparticles, has been performed to achieve a release which can be better controlled in comparison to uncoated and LBL coated nanoparticles (1 bilayer (1 BL) and 2 bilayer). On the other hand, $CaCO_3$ nanoparticles being mesoporous in nature can be loaded with macromolecules like enzymes which can serve as efficient matrix for the preparation of biosensors. These findings suggest that the gelatin/$CaCO_3$ nanoparticles inside alginate matrix are superior candidates for the encapsulation of drug/macromolecules owing to the biocompatible nature of alginate. Such 'nano-in-micro' matrices can be used for drug delivery, tissue engineering and biosensor development.

Acknowledgements

We would like to acknowledge CSIR, India for funding this project. Authors would also like to acknowledge Nicomp® particle sizing systems for particle sizing of $CaCO_3$ nanoparticles and Ca–alginate microspheres.

References

Avella, M., Errico, M., & Martuscelli, E. (2001). Novel PMMA/$CaCO_3$ nanocomposites abrasion resistant prepared by an in situ polymerization process. *Nanotechnology Letters*, *1*, 213.

Azarmi, S. (2006). Optimization of a two-step desolvation method for preparing gelatin nanoparticles and cell uptake studies in 143B osteosarcoma cancer cells. *Journal of Pharmacy and Pharmaceutical Science*, *9*(1), 124–132.

Bajpai, A. K., & Choubey, J. (2006). Design of gelatin nanoparticles as swelling controlled delivery system for chloroquine phosphate. *Journal of Material Science and Material Medicine*, *17*, 345–358.

Balthasar, S., Michaelis, K., Dinauer, N., Von Briesen, H., Kreuter, J., & Langer, K. (2005). Preparation and characterisation of antibody modified gelatin nanoparticles as drug carrier system for uptake in lymphocytes. *Biomaterials*, *26*(15), 2723–2732.

Bugarski, B., Smith, J., Wu, J., & Goosen, M. F. A. (1993). Methods for animal cell immobilization using electrostatic droplet generation. *Biotechnology Techniques*, *7*(9), 677–682.

Cameroni, R. (1999). Dynamic dialysis for the drug release evaluation from doxorubicin–gelatin nanoparticle conjugates. *International Journal of Pharmaceutics*, *180*, 23–30.

Casone, M. G. (2002). Gelatin nanoparticles produced by simple W/O emulsion as delivery system for methotrexate. *Journal of Material Science: Materials in Medicine*, *13*, 523–526.

Chavanpatil, M. D., Khdair, A., & Panyam, J. (2007). Polymer–surfactant nanoparticles for sustained release of water-soluble drugs. *Journal of Pharmaceutical Science*, *96*, 803–810.

Connick, W. J. (1983). Controlled release of bioactive materials using alginate gel beads. US Patent Office, Patent No. 4,401,456.

De Vos, P., De Haan, B. J., & Van Schilfgaarde, R. (1997). Upscaling the production of microencapsulated pancreatic islets. *Biomaterials*, *18*(16), 1085–1090.

Gorna, K., & Hund, M. (2008). Amorphous calcium carbonate in form of spherical nanosized particles and its application as fillers for polymers. *Materials Science and Engineering*, *477*(1–2), 217–225.

Jayant, R., & Srivastava, R. (2007). Dexamethasone release from uniform sized nano-engineered alginate microspheres. *Journal of Biomedical Nanotechnology*, *3*(3), 245–253.

Jian-ming, S., Yong-zhong, B., Zhi-ming, H., & Zhi-xue, W. (2004). Preparation of poly (methyl methacrylate)/nanometer calcium carbonate composite by in-situ emulsion polymerization. *Journal of Zhejiang University: Science A*, *5*(6), 709–713.

Joshi, A. B., & Srivastava, R. (2009). Polyelectrolyte coated calcium carbonate microparticles as templates for enzyme encapsulation. *Advanced Science Letters*, *2*, 1–8.

Kawaguchi, H., Hirai, H., Sakai, K., Sera, S., Nakajima, T., Ebisawa, Y., & Koyama, K. (1992). Crystallization of inorganic compounds in polymer solutions. I. Control of shape and form of calcium carbonate. *Colloid and Polymer Science*, *270*(12), 1176–1181.

Kwok, K. K., Groves, M. J., & Burgess, D. J. (1991). Production of 5–15 micron diameter alginate–polylysine microcapsules by an air atomization technique. *Pharmaceutical Research*, *8*(3), 340–344.

Lencki, R. W. J., Neufeld, R. J. and Spinney, T. (1989). Method of producing microspheres. US Patent Office, Patent No. 4,822,534.

Lu, Z., Yeh, T., Tsai, M., Au, J. L.-S., & Wientjes, M. G. (2004). Paclitaxel loaded gelatin nanoparticles for intravesical bladder cancer therapy. *Clinical Cancer research*, *10*, 7677–7684.

Ma, X., & Zhou, B. (2008). Study on $CaCO_3$/PMMA nanocomposite microspheres by soapless emulsion polymerization. *Colloids and Surfaces A: Physicochemical and Engineering Aspects*, *312*(2–3), 190–194.

Moghadam, H., & Samimi, M. (2008). Electro-spray of high viscous liquids for producing mono-sized spherical alginate beads. *Particuology*, *6*(4), 271–275.

Rahman, Z., Kohli, K., Khar, R. K., Ali, M., Charoo, N. A., & Shamsher, A. A. (2006). Characterization of 5-fluorouracil microspheres for colonic delivery. *AAPS PharmSciTech*, *7*, 47–58.

Ribeiro, C. C., Barrias, C. C., & Barbosa, M. A. (2004). Calcium phosphate–alginate microspheres as enzyme delivery matrices. *Biomaterials*, *25*(18), 4363–4373.

Saxena, A. (2005). Effect of molecular weight heterogeneity on drug encapsulation efficiency of gelatin nano-particles. *Colloids and Surfaces B: Biointerfaces*, *45*, 42–48.

Sheu, T. Y., & Marshall, R. T. (1993). Microencapsulation of lactobacilli in calcium alginate gels. *Journal of Food Science*, *54*(3), 557–561.

Stormo, K. E., & Crawford, R. L. (1992). Preparation of encapsulated microbial cells for environmental applications. *Applied and Environmental Microbiology*, *58*(2), 727–730.

Su, J., Tao, X., Xu, H., & Chen, J. F. (2007). Facile encapsulation of nanoparticles in nanoorganized bio-polyelectrolyte microshells. *Polymer*, *48*(26), 7598–7603.

Tissot, I., Novat, C., Lefebvre, F., & Bourgeat-Lami, E. (2001). Hybrid latex particles coated with silica. *Macromolecules*, *34*, 5737.

Tonnesen, H. H., & Karlsen, J. (2002). Alginate in drug delivery systems. *Drug Development and Industrial Pharmacy*, *28*, 621–630.

Volodkin, D. V., & Petrov, A. I. (2004). Matrix polyelectrolyte microcapsules: New system for macromolecule encapsulation. *Langmuir*, *20*(8), 3398–3406.

Wang, Y., Chen, H., Ye, C., & Hu, Y. (2008). Synthesis and characterization of CdTe quantum dots embedded gelatin nanoparticles via a two-step desolvation method. *Material Letters*, *62*, 3382–3384.

Wona, Y., & Kim, Y. (2008). Recombinant human gelatin nanoparticles protein drug carrier. *Journal of Controlled Release*, *127*(2), 154–161.

Yang, Y., Kong, X., Kan, C., & Sun, C. (1999). Encapsulation of calcium carbonate by styrene polymerization. *Polymers for Advanced Technologies*, *10*, 54.

Zhao, Q., Han, B., Wang, Z., Gao, C., Peng, C., & Shen, B. J. (2007). Hollow chitosan–alginate multilayer microcapsules as drug delivery vehicle: Doxorubicin loading and in vitro and in vivo studies. *Nanomedicine: Nanotechnology, Biology, and Medicine*, *3*, 63–74.

Zheng, C. H., & Gao, J. Q. (2004). A protein delivery system: Biodegradable alginate–chitosan–poly(lactic-co-glycolic acid) composite microspheres. *Biochemical and Biophysical Research Communications*, *323*(4), 1321–1327.

Zwiorek, K. (2004). Gelatin nanoparticles as a new and simple gene delivery system. *Journal of Pharmacy and Pharmaceutical Science*, *7*(4), 22–28.